The Astrophysical Journal Letters, 868:L7 (6pp), 2018 November 20 https://doi.org/10.3847/2041-8213/aaedac

Satellite Galaxies in the Illustris-1 Simulation: Poor Tracers of the Mass Distribution

Tereasa G. Brainerd
Boston University, Department of Astronomy, 725 Commonwealth Avenue, Boston, MA 02215, USA; brainerd@bu.edu
Received 2018 August 8; revised 2018 October 29; accepted 2018 October 30; published 2018 November 15

Abstract

Number density profiles are computed for the satellites of relatively isolated host galaxies in the Illustris-1 simulation. The mean total mass density of the hosts is well fitted by a Navarro–Frenk–White (NFW) profile. The number density profile for the complete satellite sample is inconsistent with NFW, and on scales $\lesssim 0.5\,r_{200}$, the satellites do not trace the hosts' mass. This differs substantially from previous results from semianalytic galaxy formation models. The shape of the satellite number density profile depends on the luminosities of the hosts and the satellites, and on the host virial mass. The number density profile for the faintest satellites is well fitted by an NFW profile, but the concentration is much less than the mean host mass density. The number density profile for the brightest satellites exhibits a steep increase in slope for host-satellite distances $\lesssim 0.1\,r_{200}$, in qualitative agreement with recent observational studies that find a steep increase in the satellite number density at small host-satellite distances. On scales $\gtrsim 0.1\,r_{200}$ the satellites of the faintest hosts trace the host mass reasonably well. On scales $\lesssim 0.4\,r_{200}$, the satellites of the brightest hosts do not trace the host mass, and the satellite number density increases steeply for host-satellite distances $\lesssim 0.1\,r_{200}$. The discrepancy between the satellite number density profile and the host mass density is most pronounced for the most massive systems, with the satellite number density falling far below that of the mass density on scales $\lesssim 0.5\,r_{200}$.

Key words: dark matter – galaxies: dwarf – galaxies: halos

1. Introduction

In Λ Cold Dark Matter (ΛCDM), dark matter halos follow a "universal" shape that is often parameterized as the Navarro–Frenk–White (NFW; Navarro et al. 1996, 1997) profile,

$$\rho(r) = \frac{\delta_c \rho_c}{(r/r_s)(1 + r/r_s)^2}, \quad (1)$$

where ρ_c is the critical density for closure of the universe and $r_s \equiv r_{200}/c$ is the scale radius. The virial radius, r_{200}, is the radius for which the mean interior halo mass density is $200\rho_c$. The concentration, c, is related to the characteristic overdensity, δ, through

$$\delta_c = \frac{200}{3}\frac{c^3}{\ln(1 + c) - c/(1 + c)}. \quad (2)$$

An important test of ΛCDM is the degree to which the dark matter halos of bright galaxies follow an NFW-like density profile. In order to directly probe the dark matter distribution around bright galaxies, a luminous tracer of the mass is necessary. In practice, small, faint satellite galaxies, in orbit around large, bright "host" galaxies, could be fair tracers of the mass, and it is the degree to which these objects trace the mass surrounding their hosts that is the subject of this investigation.

The degree to which observed satellite galaxies trace their hosts' mass is not settled. Budzynski et al. (2012) found that the number density profile for satellites in groups and clusters was well fitted by an NFW profile, but the concentration of the satellite distribution was a factor ∼2 lower than expected for the dark matter. In another cluster study, Wang et al. (2018) compared the mass density profile obtained from weak lensing to the satellite distribution and concluded that both profiles were well fitted by NFW, with the satellites tracing the mass. Nierenberg et al. (2012) concluded that satellites of massive galaxies ($M_* > 3 \times 10^{10}\,M_\odot$) traced the mass distribution well. Similarly, Guo et al. (2013) concluded that, with the exception of small differences at small radii and low luminosity, the satellite number density profile for isolated host galaxies was a good tracer of the mass. Wang et al. (2014) found that the satellites of relatively isolated host galaxies with stellar masses $M_* > 10^{11}\,M_\odot$ had a spatial distribution that was less concentrated than would be expected for the hosts' dark matter halos, while the satellites of less massive hosts had steeper density profiles that agreed well with the expected dark matter distribution. Tal et al. (2012) found that, on scales $\gtrsim 270$ kpc, the number density profile for the satellites of luminous red galaxies (LRGs) was well fitted by NFW. On small scales, however, Tal et al. (2012) found a distinct upturn in the satellite number density profile that is inconsistent with NFW. Further, Watson et al. (2012) and Piscionere et al. (2015) concluded that the small-scale ($\lesssim 40\,h^{-1}$ kpc) clustering of bright satellite galaxies ($M_r < -20$) was consistent with a number density profile that was much steeper than NFW.

In the theoretical regime, the degree to which satellites trace their hosts' mass is also not settled. Gao et al. (2004) combined a semianalytic galaxy formation model ("SAM") with high-resolution N-body simulations of the formation of massive galaxy clusters and concluded that luminous galaxies trace the cluster mass well. From numerical hydrodynamics simulations, Nagai & Kravtsov (2005) concluded that the concentration of the satellite distribution inside clusters was less than that of the dark matter. Sales et al. (2007, hereafter SNLWC) computed the number density profile for satellite galaxies in the Millennium simulation (MS; Springel et al. 2005) using a luminous galaxy catalog obtained from a SAM. SNLWC focused on relatively isolated host galaxies at $z = 0$, the vast majority of which were central galaxies within the surrounding dark matter distribution. SNLWC concluded that (i) the satellite number density profile was well fitted by NFW, (ii) the shape of the satellite number density profile did not depend strongly on the luminosity of the host galaxy or its halo virial mass, and

(iii) the distribution of the satellite galaxies was similar to that of the dark matter, but slightly less concentrated. Wang et al. (2014) computed number density profiles for satellite galaxies in the MS and the Millennium-II simulations (MS-II; Boylan-Kolchin et al. 2009), where the luminous galaxy catalog was obtained from a SAM. Wang et al. (2014) found that the satellites of relatively isolated host galaxies traced the mass distribution of the hosts' halos well and there was little dependence of the satellite number density profile on the physical properties of the hosts. Ye et al. (2017) explored the spatial distribution of satellites with large stellar masses ($\geqslant 10^9\,h^{-1}\,M_\odot$) in the hydrodynamical Illustris-1 simulation (Vogelsberger et al. 2014a; Nelson et al. 2015). At $z = 0$, Ye et al. found that for halos with virial masses $10^{12}\,h^{-1}\,M_\odot < M_{200} < 10^{14}\,h^{-1}\,M_\odot$, the dark matter mass within $\lesssim 0.4 r_{200}$ was better traced by satellites with a high satellite-to-host mass ratio than it was by satellites with a low satellite-to-host mass ratio. Ágústsson & Brainerd (2018) investigated the spatial distribution of satellite galaxies in the MS that were selected using redshift space criteria and found that the satellite distribution was a good tracer of the halos of red hosts, but the satellite distribution around blue hosts was roughly twice as concentrated as the hosts' halos.

Here, the hydrodynamical Illustris-1 simulation is used to obtain the number density profiles for the satellites of relatively isolated host galaxies. The key questions that are addressed are (1) the degree to which satellite galaxies trace the mass distribution and (2) how the shape of the satellite number density profile compares to the shape obtained previously from SAMs. The paper is organized as follows. The host and satellite selection criteria and the properties of the sample are presented in Section 2. Satellite number density profiles and host galaxy mass density profiles are presented in Section 3. A summary and discussion of the results are presented in Section 4.

2. Host-satellite Sample

Illustris-1 followed the growth of structure in a ΛCDM universe using $\Omega_m = 0.2726$, $\Omega_\Lambda = 0.7274$, $\Omega_b = 0.0456$, $\sigma_8 = 0.809$, $n_s = 0.963$, and $H_0 = 70.4\,\mathrm{km\ s^{-1}\ Mpc^{-1}}$. The simulation volume was a cubical box with periodic boundary conditions and comoving sidelength $L = 106.5$ Mpc. A total of 1820^3 dark matter particles of mass $6.3 \times 10^6\,M_\odot$ and 1820^3 hydrocells with initial baryonic mass resolution of $1.26 \times 10^6\,M_\odot$ were used. Here, only the $z = 0$ time step is used, for which the force softening length is $\epsilon_{dm} = 710$ pc, the smallest hydrodynamical gas cells are 48 pc in extent, and there are ∼40,000 luminous galaxies.

Host galaxies were obtained using the criteria adopted by SNLWC. Host galaxies have absolute magnitudes $M_r < -20.5$ and, within a radius of 1 $\mathrm{h^{-1}\,Mpc}$ centered on the host, are surrounded *only* by companions at least two magnitudes fainter than the host. Host galaxies must also have at least one companion (i.e., a satellite galaxy) within r_{200}. In addition, Illustris-1 hosts were required to be located at the centers of their friends-of-friends halos. In SNLWC, the satellite galaxies were restricted to objects with $M_r < -17$ due to the MS resolution limit. In Illustris-1 the resolution is such that satellites as faint as $M_r = -14.5$ can be resolved (see, e.g., Vogelsberger et al. 2014b) and so these additional faint satellites are also included here. Imposing these criteria results in a total of 1025 Illustris-1 host galaxies with at least one satellite within r_{200}. The total number of satellites within r_{200} of all host galaxies is 4546. Within r_{200}, the number of satellites for a given host ranges from 1 to 306, with a median of 2. The median host virial mass is $M_{200}^{\mathrm{host}} = 10^{12}\,M_\odot$, the median host absolute magnitude is $M_r^{\mathrm{host}} = -21.8$, and the median host stellar mass is $M_*^{\mathrm{host}} = 3.2 \times 10^{10}\,M_\odot$. The median host stellar mass is ∼2100 times larger than the median satellite stellar masses ($M_*^{\mathrm{sat}} = 1.5 \times 10^7\,M_\odot$), and the median host-satellite luminosity ratio is ∼2500. Because the host galaxies were selected using the same criteria, the Illustris-1 host virial mass distribution is similar to that in SNLWC (see their Figure 2). Figure 1 summarizes various properties of the sample.

3. Density Profiles

Density profiles for the satellite distribution (i.e., the mean satellite number density) and the mass surrounding the host galaxies, including both baryonic and dark matter, were computed. Following SNLWC, the density profiles were normalized by their values at $x \equiv r/r_{200} = 1$. Error bars were computed using bootstrap resampling and are omitted from figures when they are comparable to or smaller than the sizes of the data points. The top panel of Figure 2 shows the normalized density profiles for the distribution of all satellite galaxies and the mean mass density for the hosts, where the mean mass density is computed as an unweighted mean over all hosts. Also shown is the best-fitting NFW profile for the unweighted mean host mass density. The unweighted mean mass density of the hosts is well fitted by an NFW profile, and the concentration of the best fit is $c = 11.9$. On scales $\lesssim 0.4\,r_{200}$, the satellite distribution does not trace the hosts' mass. In addition, due to the inflection around $x = 0.2\,r_{200}$, the mean satellite number density cannot be fitted by an NFW profile.

The middle panel of Figure 2 shows the density profiles for the brightest satellites ($M_r < -17$), corresponding to the satellites in SNLWC, together with the density profiles for the faint satellites that are resolved in Illustris-1 but not the MS. Since the median absolute magnitude of the Illustris-1 satellites is $M_r^{\mathrm{med}} = -16.8$, division of the satellites into those with $M_r < -17$ and those with $M_r > -17$ effectively splits the sample in half. From the middle panel of Figure 2, the Illustris-1 satellites that are comparable in luminosity to SNLWC's satellites have a number density profile that cannot be fitted by an NFW profile, again due to the steep upturn at small host-satellite separations. In contrast, the number density profile for Illustris-1 satellites with $M_r > -17$ is well fitted by an NFW profile. However, the concentration of the best-fitting NFW profile for the number density of the faintest satellites, $c = 1.8$, is a factor of 6.5 less than that of the unweighted mean host mass density. That is, the faintest satellites, while following an NFW profile, have a spatial distribution that is significantly less concentrated than the underlying mass.

Since the number of satellites per host increases with host virial mass, more massive hosts contribute a greater number of satellites to the satellite number density profile than do less massive hosts. To assess the effects of this on the degree to which the satellites trace the host mass density, the bottom panel of Figure 2 shows the satellite number density profiles of the faint and bright satellites (i.e., from the middle panel of Figure 2), along with the mean host mass density computed in two ways: an unweighted mean and a weighted mean in which the weights correspond to the number of satellites within r_{200}. From the bottom panel of Figure 2, the mean host mass density, weighted by the number of satellites for each host, results in a

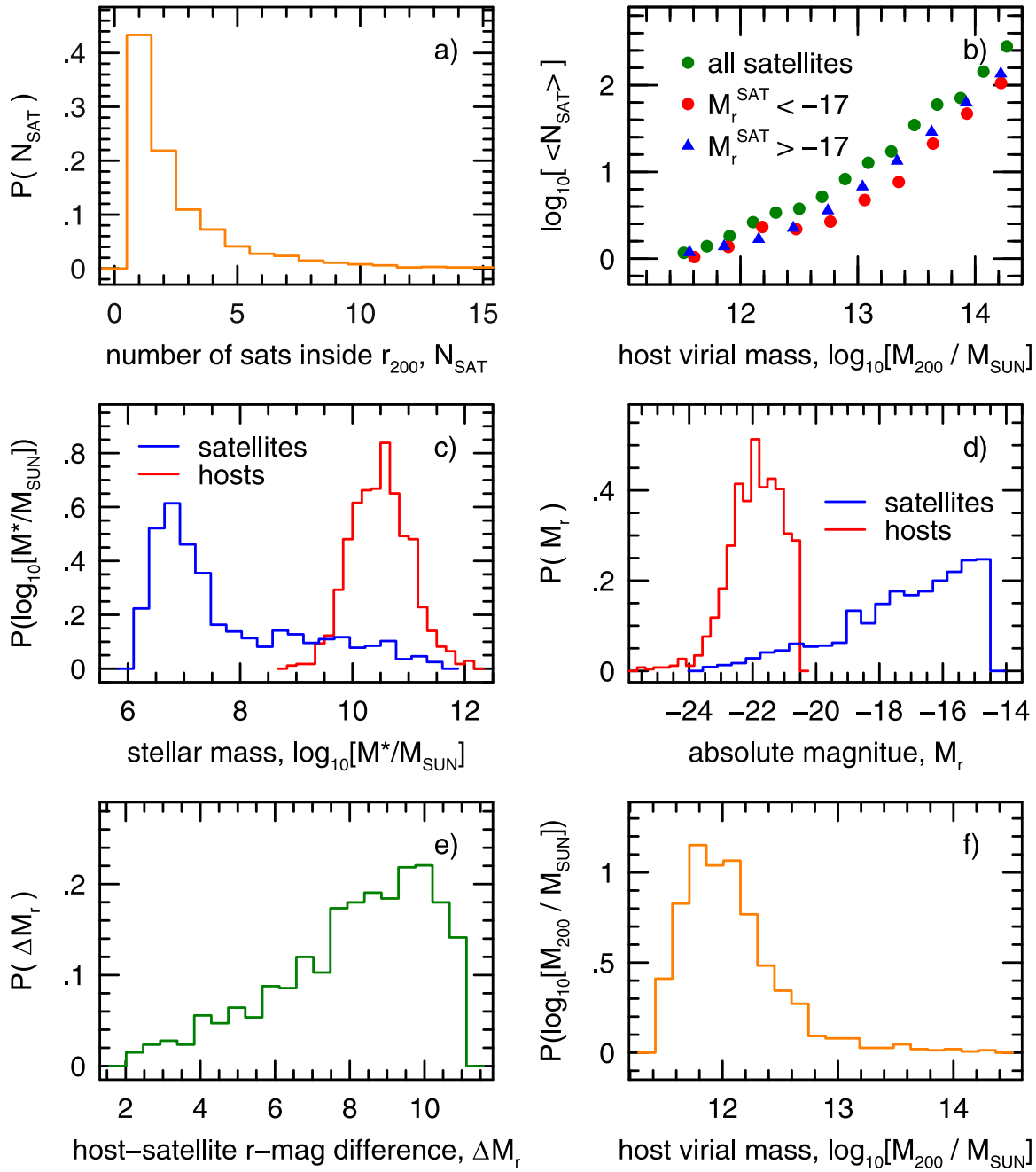

Figure 1. Properties of the sample: (a) distribution of the number of satellites within r_{200}, (b) number of satellites within r_{200} as a function of host virial mass, (c) stellar mass distributions for hosts and satellites, (d) absolute r-band magnitude distributions for hosts and satellites, (e) distribution of host-satellite r-band absolute magnitude differences, and (f) host virial mass distribution.

less concentrated mean host mass density profile ($c = 7.3$ for the weighted mean versus $c = 11.9$ for the unweighted mean). This does not, however, significantly affect the overall disagreement between the satellite number density profile and the mean host mass density profile.

Figure 3 shows the dependence of the satellite number density profiles on host luminosity, with the results for the brightest one-third of the hosts ($M_r < -22.5$) shown in the top panel and the results for the faintest one-third of the hosts ($M_r > -21.5$) shown in the bottom panel. As in Figure 2, the satellites are split into "faint" and "bright" samples, and both unweighted and weighted mean host mass density profiles are shown. Since the number of satellites per host varies little for the hosts in the top and bottom panels of Figure 2, the weighted and unweighted mean host mass densities in these panels are essentially identical. In the case of the most luminous hosts (for which the number of satellites per host varies significantly), the weighted mean host mass density is somewhat less concentrated than the unweighted mean. From Figure 3, it is clear that in no case do the satellites trace the host mass over all scales that are resolved by the simulation. (Note that the smallest host-satellite separation shown in Figure 3, $r/r_{200} \sim 0.06$, corresponds to $\sim 10\epsilon_{dm}$ for the host with the smallest virial radius, $r_{200} = 123$ kpc.) The shape of the satellite number density profile depends on host luminosity, and it deviates most significantly from the host mass density in the case of the most

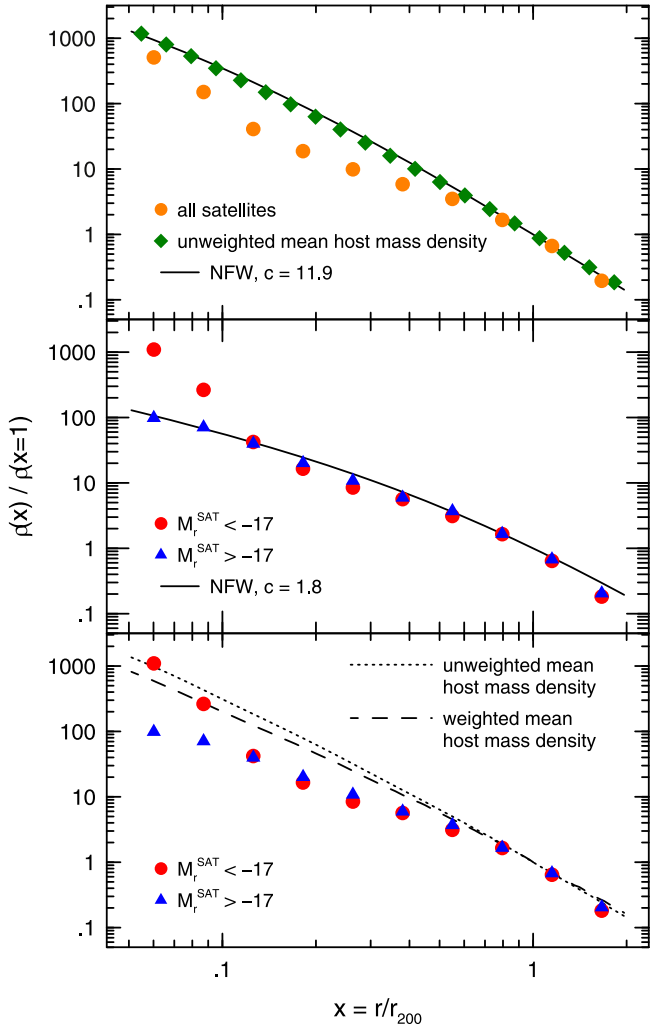

Figure 2. Normalized satellite number density profiles and host mass density profiles. Top: all satellites (orange circles), host mass density computed as an unweighted mean (green diamonds), and best-fitting NFW profile for the host mass density (solid black line). Middle: satellites with M_r comparable to the satellites in SNLWC (red circles), satellites with M_r fainter than the satellites in SNLWC (blue triangles), and best-fitting NFW profile for the faint satellites. Bottom: faint and bright satellites from the middle panel, and host mass density computed as both an unweighted mean and a weighted mean where the weights correspond to the number of satellites per host.

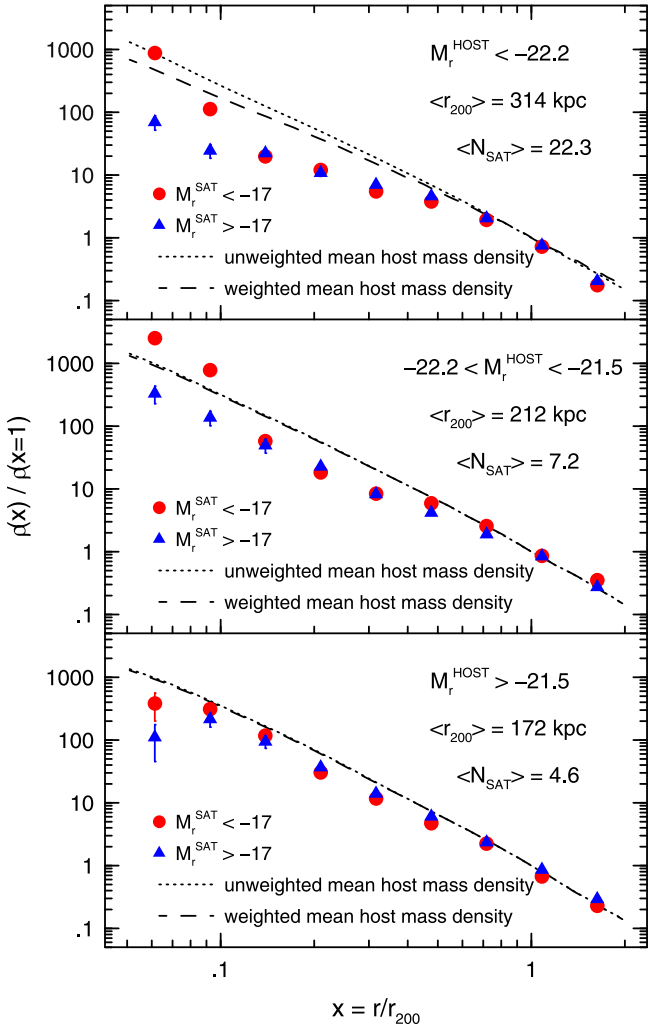

Figure 3. Normalized satellite number density profiles and host mean mass density profiles as a function of host luminosity. Satellites are divided in luminosity as in Figure 2. Unweighted means and means weighted by the number of satellites per host are shown for the host mass density. Top: brightest hosts ($M_r < -22.2$; 355 hosts). Middle: hosts with $-22.2 \leqslant M_r \leqslant -21.5$ (301 hosts). Bottom: faintest hosts ($M_r > -21.5$; 369 hosts).

luminous hosts. In the case of the faintest hosts, the satellites trace the host mass reasonably well on scales $\gtrsim 0.1\, r_{200}$. The satellite number density profile of the faintest hosts shows little dependence on satellite luminosity. For the brighter host galaxies, however, the number density of the bright satellites exceeds that of the faint satellites on scales $\lesssim 0.1\, r_{200}$.

Figure 4 shows the dependence of the satellite number density profile on host virial mass. The top panel shows the most massive 9% of the systems, for which the deviation of the satellite number density profile from the host mass density is particularly pronounced. The other panels show lower-mass hosts, split into two samples of roughly equal size. As in Figure 3, the host mass density profiles were computed as both unweighted means and means weighted by the number of satellites per host. It is only in the case of the most massive hosts that weighting the mean host mass density by the number of satellites has any noticeable effect on the resulting density profile, and it does not significantly affect the degree to which the satellites trace the host mass density. The number density profiles for the satellites of the most massive systems show little dependence on satellite luminosity. In the case of the less massive hosts, the number density of the bright satellites exceeds that of the faint satellites on scales $\lesssim 0.1\, r_{200}$.

4. Summary and Discussion

The analysis above shows that the number density profiles for Illustris-1 satellite galaxies differ substantially from the number density profiles of similar systems obtained using SAMs. The most striking difference is that on scales $\lesssim 0.4\, r_{200}$ the complete sample of Illustris-1 satellites does not trace the surrounding mass density of the hosts. The number density profile of the brightest satellites ($M_r < -17$, comparable to SNLWC's satellites) cannot be fitted by an NFW profile due to a steep increase in the slope of the number density profile for host-satellite separations $r \lesssim 0.1\, r_{200}$. The number density profile of the faintest satellites ($M_r > -17$) is well fitted by an NFW profile, but the concentration of the best-fitting NFW profile is much lower than the concentration of the mean host mass density. That is, the distribution of faint

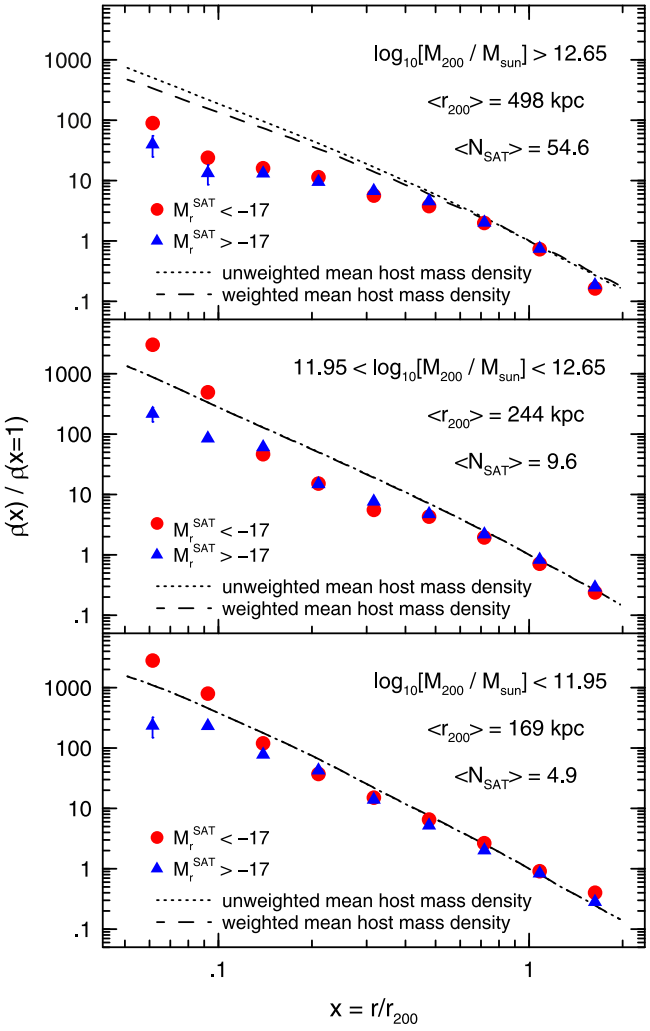

Figure 4. Normalized satellite number density profiles and host mean mass density profiles as a function of host virial mass. Satellites are divided in luminosity as in Figure 2. Unweighted means and means weighted by the number of satellites per host are shown for the host mass density. Top: most massive hosts ($M_{200} > 4.5 \times 10^{12}\,M_{\odot}$; 92 hosts). Middle: hosts with $8.9 \times 10^{11}\,M_{\odot} \leqslant M_{200} \leqslant 4.5 \times 10^{12}\,M_{\odot}$ (472 hosts). Bottom: least massive hosts ($M_{200} < 8.9 \times 10^{11}\,M_{\odot}$; 461 hosts).

satellites is significantly less concentrated than is the mass surrounding the hosts. Weighting the mean host mass density by the number of satellites per host does not affect this conclusion. In addition, the shapes of the satellite number density profiles for Illustris-1 satellites show a clear dependence on host luminosity and virial mass that was not seen by SNLWC.

A key difference between the Illustris-1 satellites and SNLWC's satellites is the methodology by which the luminous galaxy catalogs were created, i.e., a hydrodynamical simulation versus a SAM. Because the luminous galaxy catalogs resulted from different techniques, some differences should be expected. In particular, significant differences might be expected to manifest on small host-satellite separations. This is due to the different ways in which satellites, orbiting near the host galaxies, are treated. Satellites in hydrodynamical simulations are followed by the simulation directly. They are tidally stripped, disrupted, and merge with their hosts on a timescale that relies on direct integration of the equations of motion. In SAMs, once satellite galaxies orbiting close to their hosts are stripped of so much dark matter that the mass of their subhalo drops below the resolution limit, the satellite can only be identified by the position and velocity of a single particle. That single particle corresponds to the most bound particle at the last time the satellite's subhalo could be resolved. Once this point is reached, the SAM merges the satellite with the host on a particular timescale. In the case of the Croton et al. (2006) SAM used by SNLWC, stripped satellites were merged with their host on a timescale set by dynamical friction. The steep upturn in the number density profile for Illustris-1 satellites with $M_r < -17$ on scales $\lesssim 0.1\,r_{200}$, which was not found by SNLWC for similar MS satellites, may indicate that the Croton et al. (2006) SAM merged satellites with their hosts faster than would have occurred if the MS had incorporated numerical hydrodynamics.

The difference in force resolution between Illustris-1 and the MS is another factor that could contribute to the differences between the density profiles found here and those found by SNLWC. However, in their study of satellite galaxies in both the MS and the MS-II (which had a force softening five times smaller than the MS and only a factor of two larger than Illustris-1), Wang et al. (2014) did not find a steep increase in the satellite number density profile for small host-satellite separations in the MS-II. Wang et al. (2014) concluded the differences between the number density profiles of observed satellites and those obtained from SAMs could be attributed to environmental effects in the SAMs being too efficient.

The steep increase in the number density profile exhibited by bright ($M_r < -17$) Illustris-1 satellites at small host-satellite separations is in qualitative agreement with the observational results of Tal et al. (2012), Watson et al. (2012), and Piscionere et al. (2015), all of which concluded that the number density profile of bright satellites increases on small scales. In their study of the satellites of LRGs (i.e., host galaxies that, on average, are much brighter than the Illustris-1 hosts), Tal et al. (2012) concluded that the steep increase in the satellite number density profile could be explained by a corresponding steep increase in the luminous mass density of the hosts on small scales. In particular, Tal et al. (2012) concluded that, on scales $r \lesssim 25$ kpc, the baryonic mass of the host galaxies accounts for $\gtrsim$50% of the total mass of the hosts. For the Illustris-1 hosts, no steep increase in the mass density profile occurs on small scales. Rather, the total mass density profile (i.e., baryonic plus dark matter) of the Illustris-1 hosts is well fitted by an NFW profile. Within a radius of 25 kpc (comparable to 10% of the median virial radius of the host sample, $r_{200}^{\rm med} = 205$ kpc), the baryonic mass fraction of the Illustris-1 hosts is ∼26%, rather than the $\gtrsim$50% obtained by Tal et al. (2012) for their LRG hosts. Given that the host galaxies in Tal et al. (2012) are much more massive than the vast majority of the Illustris-1 hosts, this difference in the small-scale baryonic mass fraction may not be significant. However, the present results do show that a steep increase in the satellite number density profile at small host-satellite separations does not require a corresponding steep increase in the host mass since, in the case of Illustris-1 satellites, the satellites simply do not trace the host mass on small scales.

The results presented here are, of course, dependent upon a particular simulation and the distribution of satellite galaxies for small host-satellite separations may be sensitive to approximations to the detailed gas physics that are adopted in the simulation. That in mind, it will be especially interesting to compare the present results to a similar analysis of the

IllustrisTNG simulations (e.g., Weinberger et al. 2017; Nelson et al. 2018; Pillepich et al. 2018), which adopted different models for the growth of supermassive black holes, galactic winds driven by stellar feedback, and AGN feedback. These modifications resulted in significant improvements of IllustrisTNG over the original Illustris Project, including a stellar mass function for the simulated galaxies that agrees with observations and a clear red–blue galaxy color bimodality that was not seen in the original Illustris Project. Other high-resolution hydrodynamical simulations to which it would be interesting to compare the present results include the EAGLE simulations (e.g., Schaye et al. 2014; Crain et al. 2015), the Magneticum simulations (Hirschmann et al. 2014; Teklu et al. 2015), and the MassiveBlack-II simulation (Khandai et al. 2015).

Insightful conversations with Patrick Koh and Masaya Yamamoto are gratefully acknowledged.

ORCID iDs

Tereasa G. Brainerd https://orcid.org/0000-0001-7917-7623

References

Ágústsson, I., & Brainerd, T. G. 2018, ApJ, 862, 169
Boylan-Kolchin, M., Springel, V., White, S. D. M., Jenkins, A., & Lemson, G. 2009, MNRAS, 398, 1150
Budzynski, J. M., Koposov, S. E., McCarthy, I. G., McGee, S. L., & Belokurov, V. 2012, MNRAS, 423, 104
Crain, R. A., Schaye, J., Bower, R. G., et al. 2015, MNRAS, 450, 1937
Croton, D. J., Springel, V., White, S. D. M., et al. 2006, MNRAS, 365, 11
Gao, L., De Lucia, G., White, S. D. M., & Jenkins, A. 2004, MNRAS, 352, L1
Guo, Q., Cole, S., Eke, V., Frenk, C., & Helly, J. 2013, MNRAS, 434, 1838
Hirschmann, M., Dolag, K., Saro, A., et al. 2014, MNRAS, 442, 2304
Khandai, N., Di Matteo, T., Croft, R., et al. 2015, MNRAS, 450, 1349
Nagai, D., & Kravtsov, A. V. 2005, ApJ, 618, 557
Navarro, J. F., Frenk, C. S., & White, S. D. M. 1996, ApJ, 462, 563
Navarro, J. F., Frenk, C. S., & White, S. D. M. 1997, ApJ, 490, 493
Nelson, D., Pillepich, A., Genel, S., et al. 2015, A&C, 13, 12
Nelson, D., Pillepich, A., Springel, V., et al. 2018, MNRAS, 475, 624
Nierenberg, A. M., Auger, M. W., Treu, T., et al. 2012, ApJ, 752, 99
Pillepich, A., Springel, V., Nelson, D., et al. 2018, MNRAS, 473, 4077
Piscionere, J. A., Berlind, A. A., McBride, C. K., & Scoccimarro, R. 2015, ApJ, 806, 125
Sales, L. V., Navarro, J. F., Lambas, D. G., White, S. D. M., & Croton, D. J. 2007, MNRAS, 382, 1901 (SNLWC)
Schaye, J., Crain, R. A., Bower, R. G., et al. 2014, MNRAS, 446, 521
Springel, V., White, S. D. M., Jenkins, A., et al. 2005, Natur, 435, 629
Tal, T., Wake, D. A., & van Dokkum, P. G. 2012, ApJL, 751, L5
Teklu, A. F., Remus, R. S., Dolag, K., et al. 2015, ApJ, 812, 29
Vogelsberger, M., Genel, S., Springel, V., et al. 2014a, Natur, 509, 177
Vogelsberger, M., Genel, S., Springel, V., et al. 2014b, MNRAS, 444, 1518
Wang, C., Li, R., Gao, L., et al. 2018, MNRAS, 475, 4020
Wang, W., Sales, L. V., Henriques, B. M. B., & White, S. D. M. 2014, MNRAS, 442, 1363
Watson, D. F., Berlind, A. A., McBride, C. K., Hogg, D. W., & Jiang, T. 2012, ApJ, 749, 83
Weinberger, R., Springel, V., Hernquist, L., et al. 2017, MNRAS, 465, 3291
Ye, J.-N., Guo, H., Zheng, Z., & Zehavi, I. 2017, ApJ, 841, 45